The Plant Cell, Vol. 25: 4580–4595, November 2013, www.plantcell.org

A γ-Glutamyl Cyclotransferase Protects *Arabidopsis* Plants from Heavy Metal Toxicity by Recycling Glutamate to Maintain Glutathione Homeostasis[C][W]

Bibin Paulose,[a] Sudesh Chhikara,[a] Joshua Coomey,[a] Ha-il Jung,[b] Olena Vatamaniuk,[b] and Om Parkash Dhankher[a,1]

[a] Stockbridge School of Agriculture, University of Massachusetts, Amherst, Massachusetts 01003
[b] Department of Crop and Soil Sciences, Cornell University, Ithaca, New York 14853

ORCID ID: 0000-0003-0737-6783 (O.P.D.).

Plants detoxify toxic metals through a GSH-dependent pathway. GSH homeostasis is maintained by the γ-glutamyl cycle, which involves GSH synthesis and degradation and the recycling of component amino acids. The enzyme γ-glutamyl cyclotransferase (GGCT) is involved in Glu recycling, but the gene(s) encoding GGCT has not been identified in plants. Here, we report that an *Arabidopsis thaliana* protein with a cation transport regulator-like domain, hereafter referred to as GGCT2;1, functions as γ-glutamyl cyclotransferase. Heterologous expression of GGCT2;1 in *Saccharomyces cerevisiae* produced phenotypes that were consistent with decreased GSH content attributable to either GSH degradation or the diversion of γ-glutamyl peptides to produce 5-oxoproline (5-OP). 5-OP levels were further increased by the addition of arsenite and GSH to the medium, indicating that GGCT2;1 participates in the cellular response to arsenic (As) via GSH degradation. Recombinant GGCT2;1 converted both GSH and γ-glutamyl Ala to 5-OP in vitro. *GGCT2;1* transcripts were upregulated in As-treated *Arabidopsis*, and *ggct2;1* knockout mutants were more tolerant to As and cadmium than the wild type. Overexpression of GGCT2;1 in *Arabidopsis* resulted in the accumulation of 5-OP. Under As toxicity, the overexpression lines showed minimal changes in de novo Glu synthesis, while the *ggct2;1* mutant increased nitrogen assimilation by severalfold, resulting in a very low As/N ratio in tissue. Thus, our results suggest that GGCT2;1 ensures sufficient GSH turnover during abiotic stress by recycling Glu.

INTRODUCTION

GSH is a major redox buffer in the eukaryotic cell. Conjugation with GSH or its oligomers [$(\gamma$Glu-Cys$)_n$-Gly] known as phytochelatins (PCs) is a well-known mechanism of detoxification of thiol-reactive heavy metals, metalloids, and xenobiotics (Cobbett et al., 1998; Marrs, 1996). The heavy metal cadmium (Cd) and the metalloid arsenic (As) are examples of elemental pollutants with a high affinity for thiols (Li et al., 2004). Arsenic pollution is widespread in the environment, and contamination of As in drinking water and food is a significant human health concern (Ayotte et al., 2003; Dhankher, 2005). The oxyanion arsenite (AsO_3^{-3}) contains As in its trivalent form (As^{+3} or As^{III}) and is highly thiol reactive. Arsenite binds to thiol-containing compounds, including γ-glutamyl Cys (γ Glu-Cys), GSH, and PCs (Shi et al., 1996). Pathways of arsenite detoxification that involve thiol conjugation have been reported in fungi, plants, and animals (Ghosh et al., 1999; Hartley-Whitaker et al., 2001; Suzuki et al., 2001; Dhankher et al., 2002; Li et al., 2004). In plants and fungi, GSH-conjugated arsenite is thought to be sequestered in the vacuole (Ghosh et al., 1999; Verbruggen et al., 2009), while animal cells excrete arsenite-$(GS)_3$ conjugates to the extracellular space (Tseng, 2009). Arsenate (AsO_4^{-3}), which contains As in its pentavalent form (As^{+5} or As^{V}), is taken up via the phosphate uptake system in plants, and it is then electrochemically reduced to arsenite (Dhankher et al., 2006; Ellis et al., 2006). The reduced form of GSH is required for the reduction of arsenate to arsenite by arsenate reductase (Liu and Rosen, 1997). Similarly, Cd hypersensitivity of *Schizosaccharomyces pombe* and *Arabidopsis thaliana* mutants deficient in either GSH or PC synthesis established the importance of GSH and PCs in Cd detoxification (Ha et al., 1999; Howden et al., 1995; Cobbett et al., 1998).

The detoxification of heavy metals by GSH conjugation results in the rapid depletion of GSH in the cytoplasm (Polhuijs et al., 1992). Under these conditions, GSH homeostasis is maintained by the γ-glutamyl cycle (Figure 1), which involves GSH synthesis and degradation, and the recycling of the component amino acids Glu, Cys, and Gly (Griffith et al., 1978). GSH synthesis involves two ATP-dependent reactions that are catalyzed by γ Glu-Cys synthase (GSH1) and GSH synthetase (GSH2). An unusual γ-glutamyl peptide bond is formed between the side-chain carboxyl group of Glu and Cys and then Gly is added to form GSH (Meister, 1988). The importance of GSH synthesis in heavy metal detoxification mechanisms involving sulfur donor ligands in plants is well established. Both *GSH1* and *GSH2* transcripts are upregulated in *Arabidopsis* treated with metal ions that have a high affinity for thiols (Xiang and Oliver, 1998). Indian mustard (*Brassica juncea*) plants overexpressing bacterial GSH1 are tolerant to Cd and accumulated 40 to 90% more Cd in the shoot (Zhu et al.,

[1] Address correspondence to parkash@psis.umass.edu.
The author responsible for distribution of materials integral to the findings presented in this article in accordance with the policy described in the Instructions for Authors (www.plantcell.org) is: Om Parkash Dhankher (parkash@umass.edu).
[C] Some figures in this article are displayed in color online but in black and white in the print edition.
[W] Online version contains Web-only data.
www.plantcell.org/cgi/doi/10.1105/tpc.113.111815

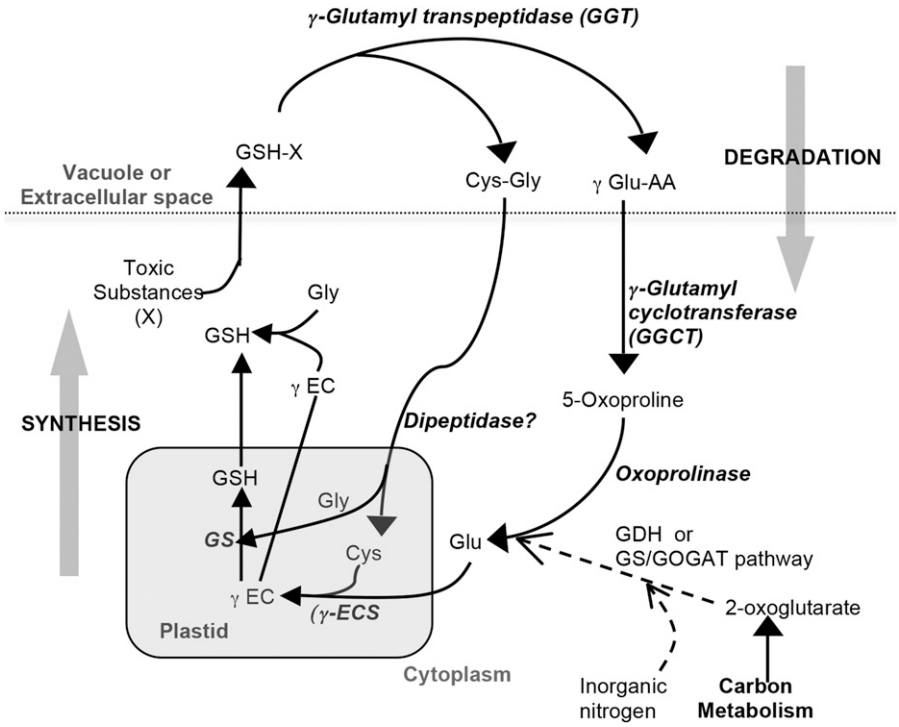

Figure 1. Predicted Pathways of the γ-Glutamyl Cycle in Plants.

The associated N assimilation pathway mentioned in Results is also shown. γ-EC, γ Glu-Cys; GS, GSH synthetase; γ Glu-AA, γ-glutamyl dipeptide; GDH, Glu dehydrogenase; GS/GOGAT, Glu synthase/Gln oxoglutarate aminotransferase.

1999). Similarly, the overexpression of bacterial GSH1 complemented arsenate sensitivity in *Arabidopsis* plants overexpressing *Escherichia coli* arsenate reductase (*ArsC*) and caused a threefold increase in As accumulation in the shoot (Dhankher et al., 2002). Improving sulfur nutrition was also found to increase tolerance to As due to elevated thiol content in plants that received higher amount of sulfur (Srivastava and D'Souza, 2009).

GSH degradation is initiated by γ-glutamyl transpeptidase (GGT), which cleaves the γ-glutamyl bond in reduced, oxidized, or conjugated forms of GSH (Figure 1). Genes encoding GGTs have been reported for many plant species, and three genes encoding functional proteins, namely, GGT1, GGT2, and GGT4, are found in *Arabidopsis* (Grzam et al., 2007; Martin et al., 2007; Ohkama-Ohtsu et al., 2008). In *Arabidopsis*, GGT1 is proposed to degrade oxidized GSH in the extracellular space, whereas GGT4 is considered to be responsible for the degradation of GSH conjugates in the vacuole (Ohkama-Ohtsu et al., 2008). Once the γ-glutamyl bond is cleaved by GGT and transferred to another amino acid, forming a γ-glutamyl dipeptide, the remaining Cys-Gly dipeptide is hydrolyzed by a dipeptidase in the cytoplasm and both amino acids are reused for further synthesis of GSH (Figure 1). The γ-glutamyl dipeptide released by GGT is processed to form 5-oxoproline (5-OP) by γ-glutamyl cyclotransferase (GGCT) and then the 5-OP is converted to Glu through an ATP-dependent reaction by oxoprolinase (Meister, 1974).

Whereas the Cys-Gly dipeptidase activity remains to be characterized in plants, the GGCT and oxoprolinase in vitro activities were reported many years ago (Rennenberg et al., 1981; Steinkamp and Rennenberg, 1987). Oxoprolinase activity that required an ATP and a divalent cation was observed in wheat (*Triticum aestivum*) germ (Mazelis and Creveling, 1978) and tobacco (*Nicotiana tabacum*; Rennenberg et al., 1981). Recently,

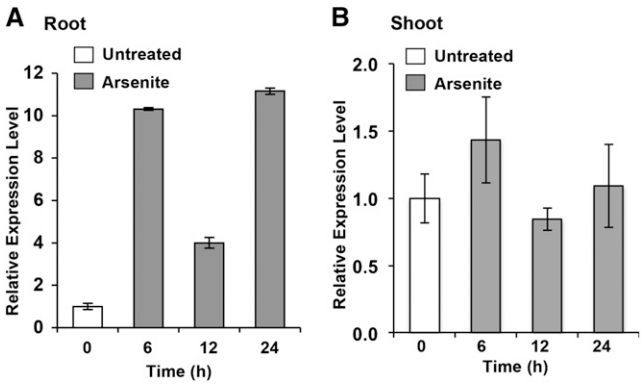

Figure 2. RT-PCR Analysis of *GGCT2;1* Expression in Response to Arsenite Treatment.

Expression analysis was performed using *GGCT2;1*-specific primers and RNA isolated from roots **(A)** and shoots **(B)** of *Arabidopsis* plants subjected to arsenite treatment. *Elongation factor* (*EF1*α) was used as an internal control. Error bars represent SE values of three replicates.

a single locus (At5g37830) coding for oxoprolinase was identified and partially characterized in *Arabidopsis* (Ohkama-Ohtsu et al., 2008). Evidence of GGCT activity in plants was first observed in tobacco suspension cultures (Steinkamp and Rennenberg, 1987). This cytoplasmic enzyme was purified and found to convert γ Glu-Met and γ Glu-Cys to 5-OP under in vitro conditions. An interesting study by Ohkama-Ohtsu et al. (2008) employing triple mutants of *Arabidopsis* deficient in GGT1, GGT4, and oxoprolinase unambiguously established the existence of GGCT. Although GGCT activity was reported many years ago, the gene(s) encoding GGCT in plants was not identified. Furthermore, the role of GGCT and oxoprolinase in detoxification of thiol-reactive pollutants, such as divalent cations (e.g., Cd^{2+}, mercury, copper, zinc, and lead) and oxyanions (e.g., AsO_3^{-3} and selenite), has not been fully investigated.

A subtracted *Crambe abyssinica* cDNA library of differentially expressed transcripts in response to As stress (Paulose et al., 2010) contained an unknown protein sequence with a ChaC (for cation transporter-associated protein) domain. Its *Arabidopsis* homolog, At5g26220, which has 76% amino acid sequence identity, possesses a cation transport regulator-like (ChaC) domain with a putative GGCT active site similar to that of human GGCT (Oakley et al., 2008). Residues forming the putative active site in human GGCT (Oakley et al., 2008) are conserved in ChaC homologs from different organisms. Interestingly, a putative active site residue, Glu-98, the mutation of which resulted in a 100% loss of function in human GGCT, is highly conserved in ChaC homologs in bacteria, fungi, plants, and mammals (see Supplemental Figure 1 online). Most eukaryotes have two ChaC homologs, ChaC1 and ChaC2, whereas *Arabidopsis* has three ChaC paralogs, two of which are similar to ChaC2 (see Supplemental Data Set 1 and Supplemental Figure 2 online). Here, we report that At5g26220 is the gene encoding GGCT in plants. Furthermore, we present evidence that the *Arabidopsis* ChaC-like protein, referred to here as GGCT2;1 because it is one of the two ChaC2 paralogs, plays a role in detoxification of heavy metals and metalloids by recycling Glu via its GGCT activity.

RESULTS

GGCT2;1 Is Upregulated in Response to Arsenite Treatment

Seven-day-old *Arabidopsis* seedlings grown in 0.5× Murashige and Skoog (MS) liquid medium were treated with 25 μM sodium arsenite for 0, 6, 12, and 24 h. A quantitative RT-PCR analysis showed that the level of *GGCT2;1* transcripts increased significantly upon arsenite treatment in roots (Figure 2). The transcript level increased more than ninefold by 6 h, and the maximum (11-fold) increase was observed 24 h after arsenite treatment. In shoots, there was no significant increase in the *GGCT2;1* transcript level (Figure 2).

GGCT2;1 Increased the Sensitivity of Transporter-Deficient *Saccharomyces cerevisiae* Strain HD9 to Arsenite and Cd

The *Saccharomyces cerevisiae* HD9 strain (Liu et al., 2002) is deficient in three transporters: an arsenite efflux transporter (ARSENICAL COMPOUND RESISTANCE3 [ACR3]), a vacuolar GS-X conjugate transporter (YEAST CADMIUM FACTOR1 [YCF1]), and a bidirectional arsenite influx/efflux transporter (FACILITATOR OF GLYCEROL TRANSPORT1). Because of the impaired arsenite efflux and vacuolar sequestration, the HD9 strain is highly sensitive to As. As a result of the YCF1 deficiency, Cd detoxification by vacuolar sequestration of the $Cd(GS)_2$ conjugate is also compromised in the HD9 strain. Therefore, this As/Cd-sensitive strain is dependent on the reactivity of GSH to decrease the toxicity of thiol-reactive toxic metals and metalloids in the cytoplasm. To test the function of GGCT2;1 in As and Cd detoxification, we heterologously expressed GGCT2;1 in *S. cerevisiae* strain HD9 and compared the As and Cd sensitivity of HD9-GGCT2;1 cells to HD9 cells expressing the pYES3 empty vector. Heterologous expression of GGCT2;1 in HD9 strain increased sensitivity to both Cd and arsenite (Figure 3A). When grown on medium without any toxic metals, both the cells containing empty vector and those transformed with GGCT2;1 grew at equal rates. However, the presence of 100 μM arsenite severely inhibited the growth of

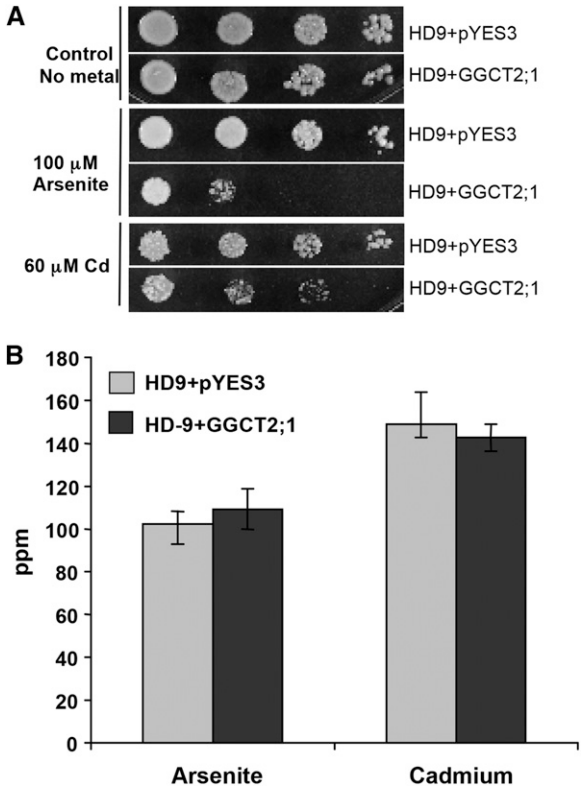

Figure 3. *Arabidopsis* GGCT2;1 Increased the Sensitivity of the HD9 (Δ*ycf1* Δ*acr3* Δ*fps1*) Triple Mutant *S. cerevisiae* Strain to Arsenite and Cd.

(A) Heavy metal assay. The 10-fold serial dilutions (left to right) of the liquid cultures of equal OD_{600} of HD9 strain expressing GGCT2;1 or pYES3 empty vector were spotted on SC medium with or without arsenite or Cd. Growth was monitored after 2 to 3 d at 30°C.

(B) Total As and Cd content in overnight cultures of HD9 cells is shown in ppm. HD9 cells containing only pYES3 empty vector were used as a control. Error bars represent SE values of four replicates.

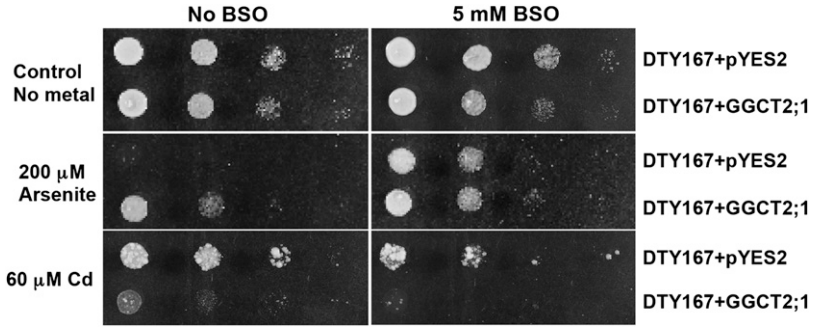

Figure 4. Heterologous Expression of GGCT2;1 in the DTY167 (Δ*ycf1*) *S. cerevisiae* Strain Results in a Cd-Sensitive and Arsenite-Tolerant Phenotype.

Growth of the DTY167 strain was affected by BSO and GGCT2;1 expression. The transformants were grown in liquid medium, and 10-fold serial dilutions of the cultures (left to right) were spotted on SC medium with or without arsenite and Cd in the presence or absence of BSO. Growth was monitored after 2 to 3 d at 30°C.

the *S. cerevisiae* cells expressing GGCT2;1, whereas the cells with an empty vector were able to survive. Similarly, in the presence of 60 μM Cd, GGCT2;1 expression inhibited cell growth significantly compared with the cells harboring only the empty vector.

To test whether GGCT2;1 increases the sensitivity of strain HD9 strain by facilitating the accumulation of toxic metals, the As and Cd contents of *S. cerevisiae* cells expressing either GGCT2;1 or empty vector were compared using inductively coupled plasma mass spectrometry (ICP-MS). There was no

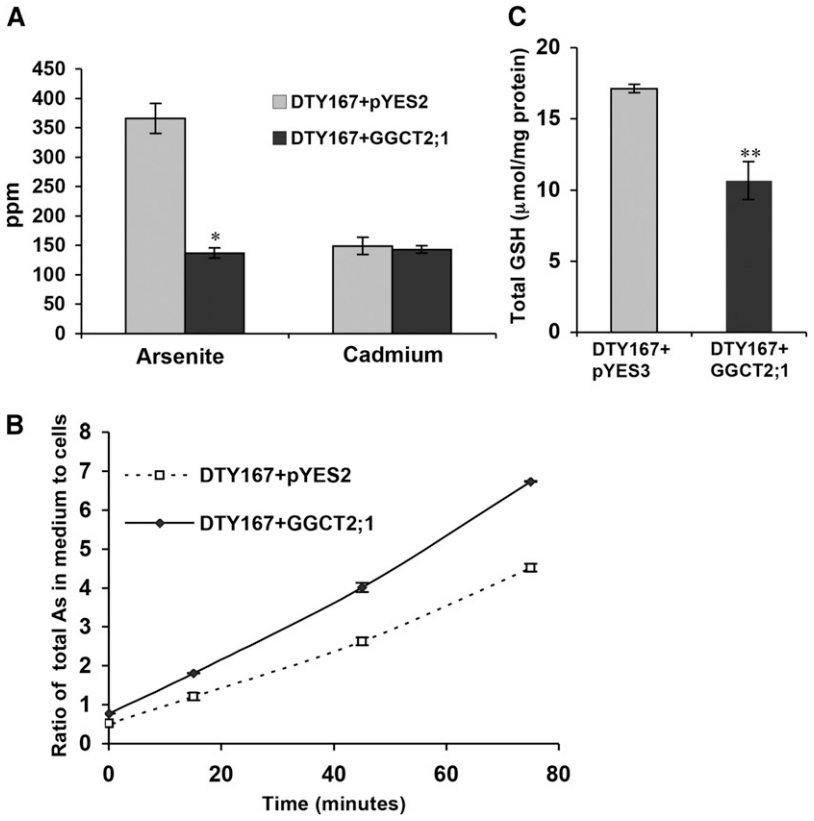

Figure 5. Heterologous Expression of GGCT2;1 in the DTY167 (Δ*ycf1*) *S. cerevisiae* Strain Results in Decreased As and GSH Accumulation.

(A) Total As and Cd content in the cells of overnight cultures of DTY167 expressing GGCT2;1 or control vector pYES2.
(B) Rate of As efflux from DTY167 cells indicated as the ratio of As in efflux buffer to the As content in the cells.
(C) Total GSH content in DTY167 cells expressing GGCT2;1 and control vector pYES2. Error bars represent SE values of four replicates. The asterisks represent a significant difference in As, Cd, and GSH content compared with cells harboring empty vector: *$P < 0.05$ and **$P < 0.01$.

significant difference in As and Cd concentrations between the cells transformed with empty vector and those expressing GGCT2;1 (Figure 3B). This suggests that the increased arsenite and Cd sensitivity of HD9 strain expressing GGCT2;1 was not due to the elevated level of toxic metals but might be caused by a significant drop in tolerance to thiol-reactive toxins, a drop contributed mostly by GSH in HD9 cells.

GGCT2;1 Expression in *S. cerevisiae* Decreased the Steady State Level of GSH

S. cerevisiae mutant strain DTY167 (Δ*ycf1*) has a defective GSH-mediated metal and metalloid detoxification pathway due to the absence of a functional ATP binding cassette transporter, YCF1, which normally transports arsenite-$(GS)_3$ or $Cd(GS)_2$ conjugates into the vacuole (Li et al., 1996). However, the arsenite extrusion pathway, mediated by ACR3, which pumps unconjugated arsenite out of the cell, is intact. The addition of buthionine sulfoximine (BSO), a specific inhibitor of GSH biosynthesis, can significantly decrease GSH levels in this strain and thus prevent the formation of arsenite-$(GS)_3$ or $Cd(GS)_2$ conjugates. To elucidate the effect of GGCT2;1 on GSH-mediated metal and metalloid tolerance, the plant transgene was overexpressed in the DTY167 mutant *S. cerevisiae* strain and its effect on the growth of the As- and Cd-sensitive DTY167 strain was observed in the presence of arsenite and Cd with or without BSO. The addition of 5 mM BSO did not affect the growth of the DTY167 mutant in the absence of arsenite and Cd (Figure 4). In the presence of 60 μM Cd, BSO increased the sensitivity of DTY167 cells containing the empty vector. Similarly, overexpression of GGCT2;1 in strain DTY167 made the cells sensitive to Cd compared with cells harboring only empty vector (Figure 4). This sensitivity was further increased by the addition of BSO.

Contrary to the Cd phenotype, both BSO and GGCT2;1 increased the tolerance of DTY167 mutants to arsenite. The mutant cells that contained empty vector failed to grow in the presence of 200 μM arsenite, and the addition of BSO rescued the cells from arsenite toxicity. Producing a phenotype similar to that produced by BSO, heterologous expression of GGCT2;1 alone was able to rescue the cells from arsenite toxicity, and the cells continued to be tolerant to arsenite in the presence of BSO. These observations suggest that the Cd tolerance in *S. cerevisiae* strain DTY167 is GSH dependent because this mutant is not able to transport Cd into the vacuole. Arsenite tolerance in this strain does not rely on GSH because the intact ACR3 extrusion pump exports unconjugated arsenite out of the cells. Regardless of this difference between the Cd and arsenite detoxification pathways, expression of GGCT2;1 mimics the effect of BSO on both the Cd and As tolerance of DTY167.

The Cd and As contents of DTY167 mutant cells were examined both in the presence and absence of GGCT2;1 expression (Figure 4). GGCT2;1 expression did not cause any difference in Cd accumulation in the DTY167 mutant cells, which is in agreement with the observations for the HD9 mutant. However, the As content in arsenite-treated DTY167 mutant cells expressing empty vector alone was almost threefold more than in cells expressing GGCT2;1 (Figure 5A). The As-tolerant phenotype of the GGCT2;1-expressing DTY167 mutant strain may have been caused by an increase in free arsenite efflux by ACR3. To test this hypothesis, we conducted As efflux assays in the DTY167 strain in the presence or absence of GGCT2;1 expression. As shown in Figure 5B, the DTY167 strain expressing GGCT2;1 showed a significantly higher rate of As transport to the efflux medium than the cells transformed with the empty vector. Since GGCT2;1 produced a phenotype similar to that produced by BSO under As toxicity, the higher rate of As efflux in the presence of GGCT2;1 most likely was due to the decrease in the steady state level of GSH. The decreased level of GSH thus resulted in an increase in unconjugated arsenite ions, which are exported by an intact ACR3 pump. To verify the low GSH content

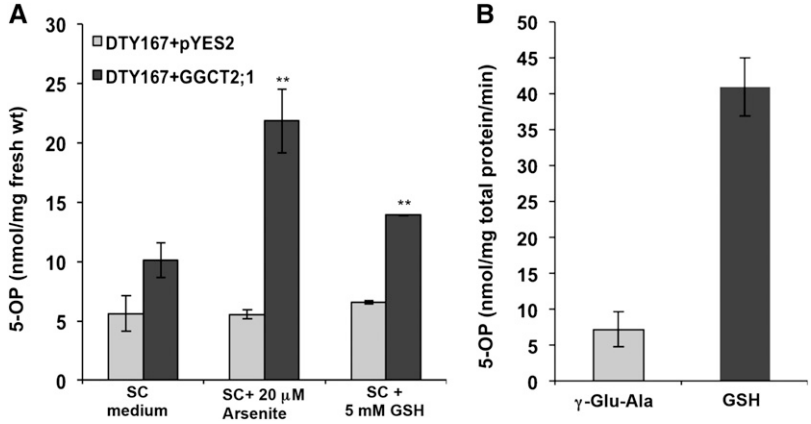

Figure 6. In Vivo and In Vitro Activity of GGCT2;1.

(A) *S. cerevisiae* cells expressing GGCT2;1 accumulate higher levels of 5-OP (5-oxoproline or pyroglutamic acid). The 5-OP content was measured in nanomoles per milligrams of fresh weight of DTY167 cells transformed with GGCT2;1 or pYES2 empty vector. Error bars represent SE values of three replicates. The asterisks represent a significant difference in 5-OP content compared with cells harboring empty vector: *$P < 0.05$ and **$P < 0.01$.
(B) In vitro GGCT activity of *Arabidopsis* GGCT2;1. Activity was measured as 5-OP produced from γ-glutamyl Ala or GSH used as substrate along with controls without enzyme.

in the presence of GGCT2;1, total GSH was extracted from the DTY167 mutant transformed with GGCT2;1 or the empty vector control and quantified by HPLC (Figure 5C). The total GSH content decreased by 40% in the GGCT2;1-expressing mutant cells compared with the cells harboring the empty vector, confirming that Cd sensitivity and arsenite tolerance in the GGCT2;1-expressing DTY167 strain was due to the lower GSH content.

GGCT2;1 Converts γ-Glutamyl Peptides to 5-OP

Heterologous expression of GGCT2;1 resulted in a significantly higher accumulation of 5-OP in the DTY strain (Figure 6A). In the synthetic complete (SC) medium without As, the expression of GGCT2;1 increased 5-OP content by nearly twofold. Addition of 20 μM arsenite to the medium resulted in a more than fourfold increase in 5-OP content in DTY167 cells expressing GGCT2;1 compared with cells transformed with empty vector. Similarly, the 5-OP content in cells transformed with *GGCT2;1* and grown in SC medium supplemented with 5 mM GSH was also significantly higher (Figure 6A). The arsenite and GSH treatments did not affect the oxoproline contents of the *S. cerevisiae* cells transformed with empty vector, indicating the existence of a balanced native γ-glutamyl cycle in yeast. However, the overexpression of GGCT2;1 caused significant accumulation of 5-OP. Under As toxicity, we presumed that the substrate for GGCT2;1 increased at a higher rate, as indicated by the accumulation of 5-OP, as a result of activation of the γ-glutamyl cycle. The significant increase in 5-OP in the GGCT2;1-expressing cells in presence of GSH further showed that the substrate for GGCT2;1 increased during GSH degradation, indicating a role for GGCT2;1 in GSH homeostasis.

In vitro GGCT activity was determined using the poly-His-tagged recombinant GGCT2;1 purified by affinity chromatography. The recombinant GGCT2;1 was able to convert γ-glutamyl Ala and GSH to 5-OP in vitro (Figure 6B). The higher rate of 5-OP formation from GSH by GGCT2;1 was particularly interesting because, in general, GGCTs accept only γ-glutamyl dipeptides as a substrate. To date, the only exception is mammalian ChaC1, which is shown to act on GSH (Kumar et al., 2012). The K_m for GSH degradation by GGCT2;1 was 1.93 mM, which was within the range of intracellular GSH concentration as observed in *Arabidopsis* cells (Fricker et al., 2000).

T-DNA Insertional Mutants of GGCT2;1 Were More Tolerant to Arsenite and Cd than Wild-Type *Arabidopsis*

The *Arabidopsis* T-DNA insertion database was searched for T-DNA insertions in the At GGCT2;1 locus, and a single line

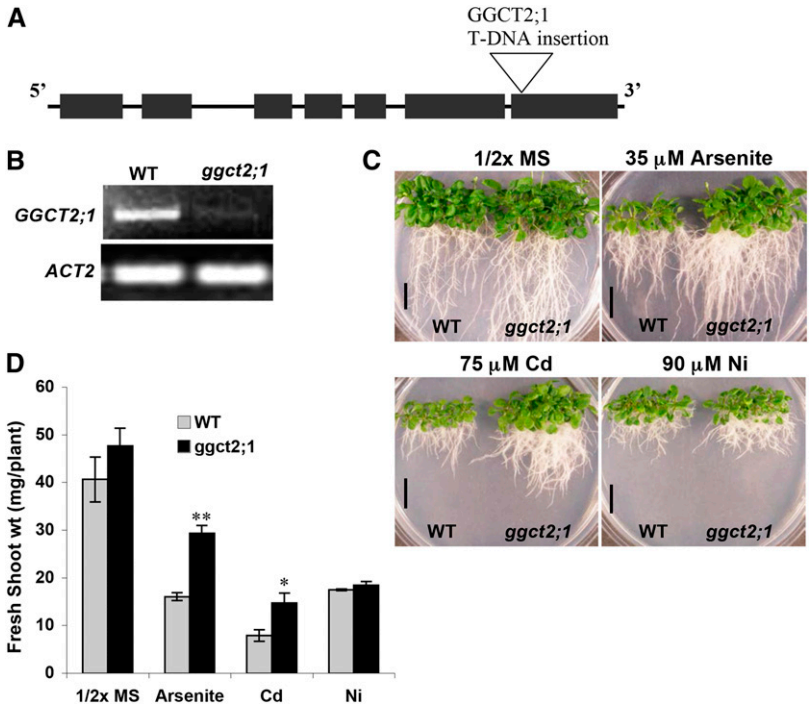

Figure 7. T-DNA Insertional Mutants of *GGCT2;1* (SALK_117578) Are Tolerant to Arsenite and Cd but Not to Ni.

(A) Structure of *GGCT2;1* showing the T-DNA insertion site. Black boxes indicate exons, and lines indicate introns.
(B) *GGCT2;1* transcript analysis in the wild type (WT) and *ggct2;1* mutant using RT-PCR and *ACT2* as control.
(C) Growth analysis of the wild type and *ggct2;1* mutants on arsenite, Cd, and Ni. Bars = 15 mm.
(D) Fresh shoot weight of wild-type and *ggct2;1* mutant plants gown on arsenite, Cd, and Ni. For biomass, the average and SE values are represented for four replicates of 12 seedlings each for wild-type and *ggct2;1* mutant lines. The asterisks represent a significant difference in biomass accumulation compared with wild-type plants: *$P < 0.05$ and **$P < 0.01$.

(SALK_117578) with a T-DNA insertion in the seventh exon was identified (Figure 7A). Homozygous plants were identified from these *ggct2;1* T-DNA insertional mutant seeds that were obtained from the ABRC. The loss of *GGCT2;1* transcript was confirmed by RT-PCR analysis. No *GGCT2;1* transcripts were detected in the T-DNA insertional mutants, whereas wild-type plants showed the presence of a 651-bp-long transcript (Figure 7B). To analyze the role of GGCT2;1 in metal tolerance, *ggct2;1* mutant seedlings were grown in 0.5× MS medium containing 35 μM arsenite, 75 μM Cd, or 90 μM nickel (Ni). The metal or metalloid treatments were based on a dose-response curve demonstrating decrease in biomass at various concentrations of these metals for wild-type *Arabidopsis* plant growth. When plated on 0.5× MS medium or the medium containing arsenite or Cd, the *ggct2;1* plants grew better than the wild-type plants (Figure 7C) and had longer roots. As shown in Figure 7D, shoot fresh weight for *ggct2;1* was nearly double that of the wild type under arsenite and Cd stress, whereas the fresh weight did not differ from that of the wild type in the absence of these toxic metals. However, there was no difference in growth *ggct2;1* and control plants grown on media containing Ni. Wild-type and *ggct2;1* plants attained almost equal fresh shoot weight when treated with 90 μm Ni. This emphasized the role of GGCT2;1 in detoxification of the thiol-reactive toxic metal(loid)s arsenite and Cd in plants. To confirm the mutant phenotypes of GGCT2;1, a second T-DNA insertional mutant (SALK_036650) with a single insertion in the 3′ untranslated region of GGCT2;1 was analyzed. This mutant also exhibited tolerance to arsenite and Cd similar to the *ggct2;1* mutant (see Supplemental Figure 3 online).

Analysis of total As showed no difference in As concentration in the roots of *ggct2;1* mutants compared with those of wild-type plants (Figure 8A). However, As concentration in the *ggct2;1* shoots was significantly lower than in wild-type plants (Figure 8B). Interestingly, this decrease in As concentration was proportional to the increase in fresh shoot weight. This finding suggests that the decrease in As concentration could be due to the dilution effect of the higher shoot biomass of the mutant plants rather than to differences in the transport of As to shoot tissues. Additionally, in agreement with the higher tolerance *ggct2;1* to arsenite and Cd toxicity, the total GSH content in the mutant was significantly higher than that of the wild-type plants (Figure 8C).

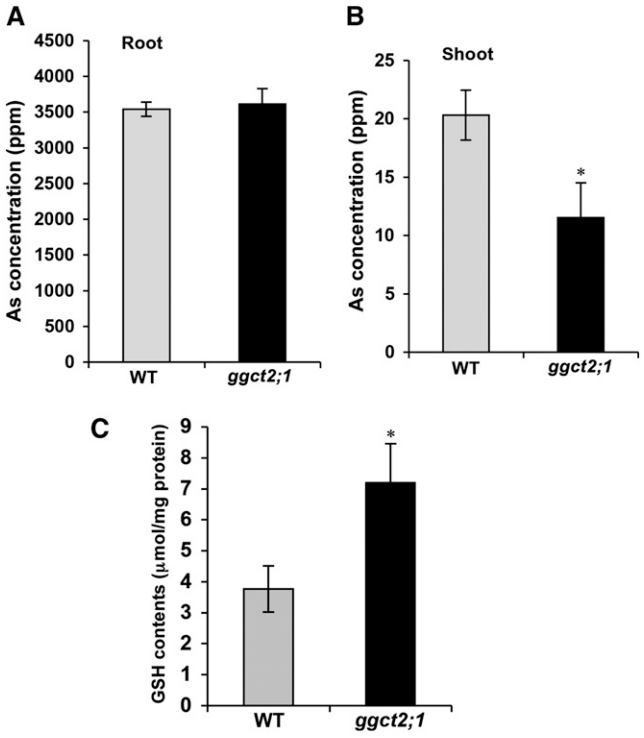

Figure 8. Analysis of Total As and GSH Contents in T-DNA Insertional Mutants of *GGCT2;1*.

(A) and **(B)** Total As content in the shoot **(A)** and root **(B)** of wild-type (WT) and *ggct2;1* mutant plants.

(C) Total GSH content in wild-type and *ggct2;1* plants. For GSH and As accumulation, the average and SE values are shown for four replicates of 25 plants each for the wild type and *ggct2;1*. The asterisks represent a significant difference in GSH and As concentration compared with wild-type plants: *$P < 0.05$ and **$P < 0.01$.

Tissue-Specific Expression of GGCT2;1 in *Arabidopsis*

To determine the pattern of native expression of GGCT2;1, β-glucuronidase (GUS) activity was assessed histochemically in transgenic *Arabidopsis* plants expressing the GUS gene under the control of the *GGCT2;1* promoter. Strong expression of GUS driven by the *GGCT2;1* promoter was observed in roots (Figure 9A). At higher magnification, the GUS expression was found to be localized mainly in the central vascular bundle in roots (Figure 9B). In leaves, GUS activity was restricted to the veins and hydathodes (Figure 9C). No activity was detected in the mesophyll tissue of the developed leaves. However, young leaves and the shoot apex showed strong GUS expression in all cells including mesophyll cells (Figure 9D). Additionally, strong GUS activity was found in the veins of sepals and in flower receptacles and in developing seeds (Figures 9E and 9F). In short, GGCT2;1 is expressed in the vascular tissue, meristem cells, and reproductive organs in *Arabidopsis* under standard growth conditions.

Overexpression of GGCT2;1 Provided Enhanced As Tolerance in *Arabidopsis*

Arabidopsis plants overexpressing *GGCT2;1* under the *Arabidopsis actin2* (*ACT2*) promoter were grown in the presence of arsenite to determine the effect of *GGCT2;1* on As detoxification. The T2 homozygous lines showed a relatively higher steady state level of *GGCT2;1* transcripts, as revealed by RT-PCR analysis (see Supplemental Figure 4 online). *Arabidopsis* plants overexpressing GGCT2;1 were more tolerant to arsenite than wild-type controls (Figure 10A). However, the observed difference in arsenite tolerance in the overexpression lines was less pronounced than in the *ggct2*;1 mutant plants. GGCT2;1

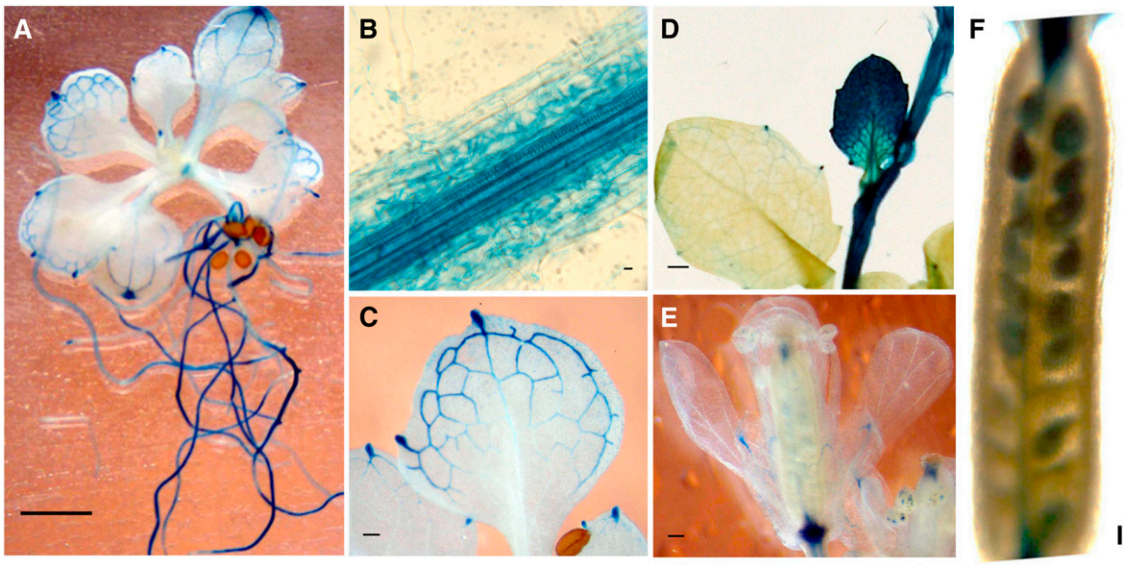

Figure 9. Tissue-Specific Expression Pattern of *GGCT2;1* as Determined by Transcriptional Fusion of the GUS Reporter Gene to the Promoter of *GGCT2;1*.

Histochemical assays showing *GGCT2;1* promoter activity in seedling **(A)**, root **(B)**, leaf vein **(C)**, developing leaves **(D)**, flowers **(E)**, and developing seeds **(F)**. Bars = 1mm.

overexpression lines had a 1.5-fold higher shoot fresh weight than did wild-type plants (Figure 10B) and had longer roots (Figure 10A).

Analysis of total GSH content in the overexpression lines and wild-type controls showed no significant difference (Figure 11A). Arsenic concentration in the shoots and roots of *Arabidopsis* wild-type and GGCT2;1 overexpression lines was analyzed by ICP-MS. The As concentration in the shoot of the overexpression lines was significantly lower than in the wild-type plants (Figure 11B), whereas in the roots the overexpression lines accumulated more As than the wild-type plants (Figure 11C).

Overexpression of GGCT2;1 Caused an Increased Level of 5-OP in *Arabidopsis*

To test the GGCT activity of GGCT2;1 in planta, 5-OP contents were estimated in two T2 homozygous GGCT2;1 overexpression lines as well as in *ggct2;1* mutants and wild-type controls. The constitutive overexpression of *GGCT2;1* under the control of *ACT2pt* resulted in the accumulation of 5-OP in *Arabidopsis* shoots up to 30-fold as compared with the wild type (Figure 12A). However, in roots of overexpression lines, less than a twofold increase in 5-OP content was observed compared with the wild type (Figure 12B). The 5-OP content in mutant plants was nearly one half of that of the wild type in both shoot and root. A very low amount of 5-OP detected in *ggct2;1* mutant indicated redundant GGCT activity in *Arabidopsis*. Thus, GGCT2;1 contributes significantly to the total GGCT activity in *Arabidopsis*.

GGCT2;1 Activity Decreases Nitrogen Requirement in *Arabidopsis* under As Toxicity

GGCTs are involved in the recycling of Glu, whose synthesis involves the assimilation of inorganic nitrogen (Forde and Lea, 2007). Therefore, we investigated the effect of GGCTs on N content under As toxicity. In the presence of As toxicity and N deficiency, there was no difference in total N content in the shoot tissues of GGCT2;1 overexpression lines, the wild type, and *ggct2;1* plants (Figure 13A). However, the *ggct2;1* mutant accumulated significantly higher amounts of N in its roots compared with the wild-type and GGCT2;1 overexpression lines (Figure 13B). Because of the impaired recycling of Glu in mutants, the high N content in the mutant roots suggests an increase in the de novo synthesis of Glu from 2-oxoglutarate by incorporating inorganic N under As toxicity. Indeed, a higher Glu synthesis was observed in the mutant when in vivo Glu synthesis was traced by isotope labeling (Figure 13C). The wild type, *ggct2;1*, and overexpression lines were grown hydroponically in 0.5× MS medium and then transferred to modified 0.5× MS that contained ^{15}N-labeled KNO_3 and 30 μM arsenite. The ^{15}N-labeled Glu in root was analyzed by HPLC–tandem mass spectrometry for up to 12 h to estimate de novo Glu synthesis. There was no difference observed up to 3 h. However, the mutant accumulated significantly higher ^{15}N labeled Glu after 6 and 12 h in roots compared with wild-type and overexpression lines (Figure 13C). In the wild type, a significant difference in ^{15}N-labeled Glu was observed only after 12 h, whereas it remained unchanged in the overexpression lines. The negative correlation between de novo Glu synthesis and GGCT2;1

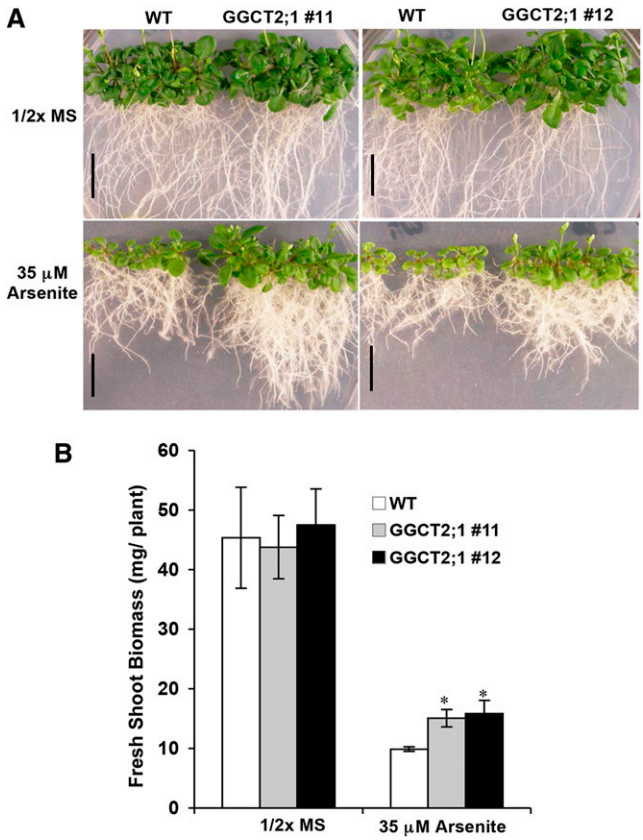

Figure 10. *Arabidopsis* Plants Overexpressing GGCT2;1 Are Tolerant to Arsenite.

(A) Growth analysis of wild-type (WT) and GGCT2;1 overexpression lines on medium containing 35 μM sodium arsenite. Bars = 15 mm.
(B) Fresh shoot weight of the wild-type and GGCT2;1 overexpression lines gown on arsenite. For biomass, the average and SE values are represented for four replicates of 12 seedlings each for wild-type and overexpression lines. The asterisks represent a significant difference compared with wild-type plants: *P < 0.05 and **P < 0.01.

expression corroborates the role of GGCT2;1 in Glu recycling during As detoxification. To confirm the effect of GGCT2;1 on N assimilation and As detoxification in roots, As accumulation per unit N content was estimated. The molar ratio of As to N was highest in At-GGCT2;1 overexpression lines followed by the wild type, with the At-*ggct2;1* mutants having the least (Figure 13D).

DISCUSSION

Effect of GGCT2;1 on Arsenite and Cd Sensitivity in *S. cerevisiae* Is Caused by a Decrease in the Steady State Level of GSH

In this study, an As-inducible gene, GGCT2;1, with GGCT activity was identified in *Arabidopsis*. Heterologous expression of GGCT2;1 in *S. cerevisiae* strains HD9 and DTY167 produced phenotypes indicative of a decreased steady state level of GSH. The decrease in GSH in strain HD9 resulted in phenotypes showing sensitivity to both Cd and arsenite toxicity. By contrast, the DTY167 strain was tolerant to arsenite, most likely due to the presence of the efflux pump ACR3 that pumps unconjugated arsenite out of the cell. Since GGCT2;1 is localized to cytoplasm, low levels of GSH in these cells could be attributed to GSH degradation by GGCT2;1.

Likewise, *S. cerevisiae* cells expressing *Arabidopsis* GGCT2;1 accumulated a significantly higher amount of 5-OP, which was further increased by the addition of either arsenite or GSH, indicating a role for GGCT2;1 in the As detoxification and GSH degradation pathways. Although *S. cerevisiae* was considered to have only a truncated version of the γ-glutamyl

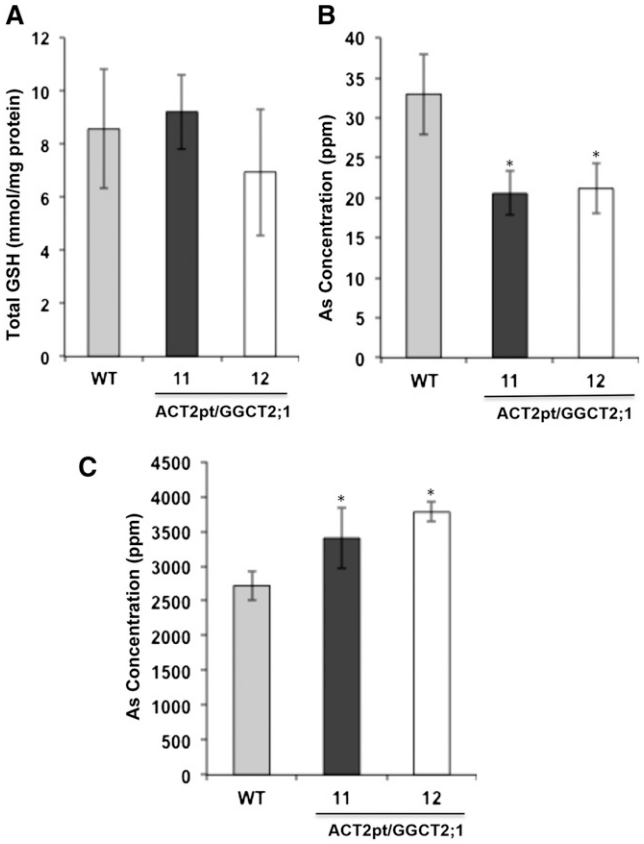

Figure 11. Analysis of Total As and GSH Contents in *Arabidopsis* Plants Overexpressing GGCT2;1.

(A) Total GSH content in wild-type (WT) and GGCT2;1 overexpression lines.
(B) and **(C)** As concentration in the shoot **(B)** and root **(C)** of wild-type and GGCT2;1 overexpression lines. For GSH and As accumulation, the average and SE values are shown for four replicates of 25 plants each for wild-type and GGCT2;1 overexpression lines. The asterisks represent a significant difference compared with wild-type plants: *P < 0.05 and **P < 0.01.

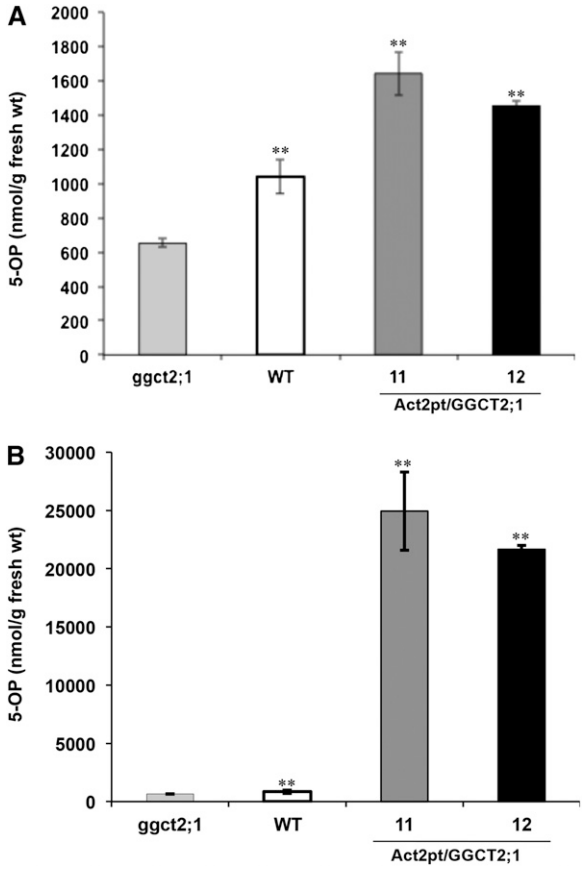

Figure 12. *Arabidopsis* Plants Overexpressing GGCT2;1 Accumulate 5-OP.

5-OP content measured in root **(A)** and shoot **(B)** of *ggct2;1* mutants, wild-type controls, and GGCT2;1 overexpression lines (11 and 12) of *Arabidopsis*. The average and SE values are shown for four replicates of 25 plants each for the wild type, *ggct2;1* mutants, and GGCT2;1 overexpression lines. The asterisks represent a significant difference in 5-OP content compared with the mutant: *$P < 0.05$ and **$P < 0.01$.

cycle (Jaspers et al., 1985), a recent report of a functional oxoprolinase in *S. cerevisiae* (Kumar and Bachhawat, 2010) suggests the existence of a complete operative γ-glutamyl cycle in *S. cerevisiae*. The results presented in this study showed that the native γ-glutamyl cycle in *S. cerevisiae* was able to maintain the steady state level of metabolites in the presence of either 20 μM arsenite or 5 mM GSH because these treatments did not change the 5-OP content in *S. cerevisiae* cells harboring the empty vector. However, the presence of GGCT2;1 altered this equilibrium by producing 5-OP faster than it could be converted to Glu in the subsequent step of the pathway, causing a net accumulation of 5-OP. Supporting these observations, the recombinant GGCT2;1 converted GSH at physiologically relevant concentrations to 5-OP.

Arsenite Tolerance Phenotypes of T-DNA Mutants and GGCT2;1 Overexpression Lines Are Due to Altered Glu Supply for GSH Homeostasis

The *ggct2;1* mutant plants were specifically tolerant to the thiol-reactive toxic elements arsenite and Cd. It is well established that the detoxification of both arsenite and Cd requires GSH and PCs in plants (Howden et al., 1995; Shi et al., 1996; Cobbet et al., 1998; Dhankher et al., 2002; Verbruggen et al., 2009). Although Ni induces oxidative stress and depletes the level of reduced GSH, it does not require GSH conjugation for its detoxification (Krämer et al., 2000). GSSG is reverted to the reduced form, primarily by GSH reductases using NADPH as an electron source, and to some extent by the NADPH-dependent thioredoxin system (Marty et al., 2009). Several studies have shown that Ni detoxification in plants is mainly through chelation with organic acids as demonstrated by a concomitant increase in malate, citrate, and oxalic acids during Ni treatments (Bhatia et al., 2005; Jócsák et al., 2005). Furthermore, NMR and x-ray spectroscopy studies showed that a major proportion of Ni was chelated with citric acid in plants (Sagner et al., 1998; Krämer et al., 2000). In accordance with these findings, steady state transcript levels of genes related to GSH metabolism responded only to thiol-reactive metal ions in *Arabidopsis* (Xiang and Oliver, 1998).

Based on the aforementioned reports and in agreement with our study, the γ-glutamyl cycle is expected to make a significant contribution only to the detoxification of thiol-reactive ions, such as arsenite and Cd, and not to that of Ni ions. Supporting its predicted role in the γ-glutamyl cycle, the *ggct2;1* mutant phenotypes were observed only under arsenite and Cd toxicity, but not under Ni toxicity. Moreover, the tissue-specific expression pattern of GGCT2;1 that was observed predominantly in roots and reproductive organs was identical to that of GGT, which catalyzes the preceding step of the γ-glutamyl cycle (Martin et al., 2007). Additionally, *oxp1* mutant *Arabidopsis* plants were unable to metabolize 5-OP and accumulated the highest amount of oxoproline in roots, flowers, and siliques (Ohkama-Ohtsu et al., 2008), indicating a highly coordinated promoter activity of the genes involved in the catabolic half of the γ-glutamyl cycle in *Arabidopsis*. This implies that the oxoprolinase activity is less in shoots and higher in roots and reproductive tissues. This observation is also supported by the surprisingly high 5-OP content in shoots of the overexpression lines, as the low level of expression of oxoprolinase might be insufficient to metabolize 5-OP formed by constitutive overexpression of GGCT2;1. The cytoplasmic localization of GGCT2;1 (see Supplemental Methods 1 and Supplemental Figure 5 online) correlates with the GGCT activity in tobacco suspension culture that localizes exclusively to the cytoplasm (Steinkamp and Rennenberg, 1987). Our results strengthen the evidence that GGCT2;1 acts in close coordination with other enzymes in the γ-glutamyl cycle.

The As- and Cd-tolerant phenotypes of the *Arabidopsis* plants deficient in GGCT2;1 can be attributed to the observed increase in GSH content. However, *Arabidopsis* plants overexpressing GGCT2;1 were tolerant to arsenite, which contradicts our findings in both the *atggct2;1* mutant and *S. cerevisiae*. A plausible explanation for this is that GSH synthesis in *Arabidopsis*

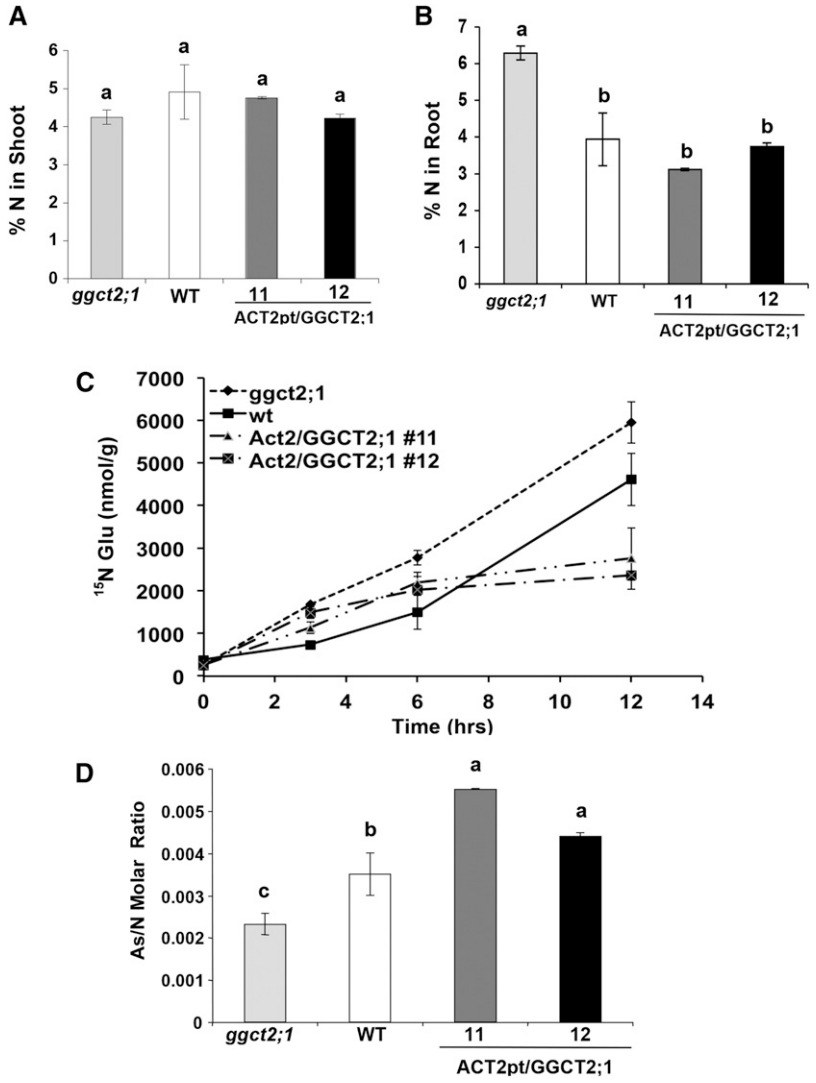

Figure 13. Analysis of *ggct2;1* Mutants, Wild-Type Controls, and GGCT2;1 Overexpression Lines under Arsenite Toxicity and N Deficiency.

(A) and **(B)** Total N measured as percentage dry weight in the shoot **(A)** and root **(B)** of plants grown in modified MS medium containing 2.5 mM N and 30 μM arsenite. WT, the wild type.

(C) De novo Glu synthesis measured as ^{15}N-labeled Glu accumulated at indicated time points after changing to a medium containing ^{15}N-labeled nitrate.

(D) Molar ratio of total As to total N in roots. Total N and As in roots was measured and plotted as their molar ratio. The average and SE values are represented for four replicates of 25 seedlings each for the wild type, *ggct2;1* mutants, and GGCT2;1 overexpression lines. Different letters indicate significant differences ($P < 0.01$) according to Duncan's new multiple range test.

is compartmentalized and that plants are therefore able to protect GSH synthesis in the presence of elevated levels of GGCT activity. In *Arabidopsis*, unlike *S. cerevisiae*, the synthesis of γ Glu-Cys is exclusively localized to the plastids (Wachter et al., 2005), whereas GSH synthetase activity has been observed in both the cytoplasm and plastids (Wachter et al., 2005; Pasternak et al., 2008). In support of both intra- and intercompartmental GSH synthesis in plants, recently identified *Arabidopsis* homologs of the *Plasmodium falciparum* chloroquine resistance transporter have been shown to import both γ Glu-Cys and GSH to the cytoplasm from plastids (Maughan et al., 2010). As a result, even in the presence of elevated levels of GGCT2;1 in the cytoplasm under As toxicity, the overexpression lines were able to maintain the required amount of GSH, most likely by increasing the synthesis of γ Glu-Cys and GSH in plastids. Additionally, the overexpression of GGCT2;1 enhanced the level of 5-OP, the precursor of Glu in the γ-glutamyl cycle.

Therefore, degradation of GSH in the cytoplasm by GGCT2;1 may provide more Glu for GSH synthesis in plastids. Isotopic labeling studies showed that the overexpression of GGCT2;1 enabled plants to recycle Glu more efficiently, which contributed to their enhanced growth under arsenite toxicity. Furthermore,

an efficient γ-glutamyl cycle in roots allows plants to accumulate more As in roots, presumably by conjugating arsenite with GSH and subsequently transporting arsenite-$(GS)_3$ conjugates to vacuoles, thereby decreasing its translocation to shoots and thus enhancing the growth of the above-ground foliage. By contrast, the *ggct2;1* mutant is deficient in recycling Glu under As toxicity; however, as demonstrated by the ^{15}N labeling studies, the decrease in recycled Glu triggers a steep increase in N assimilation, resulting in high nitrogen requirement and hence higher biomass.

Physiological Significance of GGCT2;1 in Plants Experiencing As Toxicity

In plants, the N assimilation pathway proceeds through Glu via the combined activity of Glu synthase (Gln oxoglutarate aminotransferase) and Gln synthetase incorporating inorganic N in ammoniacal form to 2-oxoglutarate (Miflin and Lea, 1976). The amino group of Glu can be transferred by aminotransferases to synthesize other amino acids (Forde and Lea, 2007), including Gly and Ser. Cys is formed by the incorporation of sulfide to the activated form of Ser, *O*-acetyl Ser (Bogdanova and Hell, 1997). Thus, apart from being a component of GSH, Glu is also required for the synthesis of the remaining amino acid components of GSH, Gly and Cys, either directly or indirectly. Furthermore, Glu is essential for many metabolic pathways, including folate metabolism (Hanson and Gregory, 2002) and tetrapyrrole biosynthesis (Yaronskaya et al., 2006). Because Glu plays a pivotal role in linking many metabolic pathways, tobacco plants were found to maintain a more or less constant level of Glu during the diurnal cycle (Geiger et al., 1998; Matt et al., 2001). In *Arabidopsis*, a major proportion of the 137 metabolites measured in rosettes, including sugars, organic acids, and all amino acids, showed significant changes in intracellular concentrations during the diurnal cycle, whereas the intracellular concentration of Glu exhibited only minor changes (Gibon et al., 2006).

However, As detoxification requires a large amount of Glu, particularly in the roots, in which the As concentration, mostly in the trivalent form, reaches up to 3000 ppm (Figure 8), which is equivalent to 40 mM. Detoxification of trivalent As requires 3 moles of GSH per mole of arsenite. Thus, the increased N uptake in *ggct2;1* mutants can be attributed to the increased de novo synthesis of Glu (Figure 13C) as a result of the need to maintain the steady state level of Glu. Because ACT2p/GGCT2;1 overexpression lines were efficient at recycling Glu, they required a low rate of de novo Glu synthesis, which resulted in decreased N uptake. On the other hand, the *ggct2;1* mutants, which were inefficient at recycling Glu in the absence of GGCT2;1, as shown by the high rate of Glu synthesis from inorganic nitrogen, became dependent on elevated N uptake to synthesize Glu. Therefore, these results suggest that GGCT2;1 participates in the recycling of Glu as part of the γ-glutamyl cycle during the detoxification of thiol-reactive toxic metals.

With their marked efficiency for recycling Glu, the GGCT2;1 overexpression lines were able to accumulate more As in roots with minimal N uptake and assimilation. Supporting the role of GGCT2;1 in Glu recycling as part of the γ-glutamyl cycle, the molar ratio of As to N in roots was lowest in mutants and highest in the overexpression lines, indicating a positive correlation between GGCT2;1 expression and As accumulation per unit N. Supporting these results that showed the importance of N in the detoxification of thiol-reactive toxins, *Arabidopsis* nitrate transporter NRT1.8 was upregulated in response to Cd stress and the *Arabidopsis* mutant deficient in NRT1.8 showed a Cd-sensitive phenotype (Li et al., 2010).

In conclusion, based on the reverse and forward genetics studies in *Arabidopsis* and heterologous expression in *S. cerevisiae* strains, the protein encoded by At5g26220, which we have named GGCT2;1, has been shown to have GGCT activity. In conjunction with other enzymes of the γ-glutamyl cycle, GGCT2;1 ensures sufficient GSH turnover during abiotic/biotic stresses that require GSH conjugation as a tolerance mechanism. By efficiently recycling Glu as part of the γ-glutamyl cycle, GGCT2;1 decreased the de novo synthesis of Glu, thereby decreasing the nitrogen requirement. Since N is the most limiting mineral nutrient for plant growth, decreasing N assimilation by manipulating the γ-glutamyl cycle holds great potential for improving crop productivity under abiotic and biotic stresses.

METHODS

Plant Materials and Growth Conditions

Arabidopsis thaliana ecotype Columbia-0 seeds were surface disinfected using 70% ethanol for 5 min followed by treatment with 30% Clorox for 30 min. Seeds were washed four times with sterile deionized water and then plated onto 0.5× MS medium (Murashige and Skoog, 1962) containing 1% Suc and 0.8% agar with pH adjusted to 5.7. For toxic metal tolerance, growth media were supplemented with arsenite, Cd, and Ni at a final concentration of 35, 75, or 90 μM, respectively. To create N-deficient medium, 0.5× MS medium was modified by decreasing the ammonium nitrate and potassium nitrate concentration to achieve a final N concentration of 2.5 mM. The absence of potassium was compensated for by adding the required amount (671 mg/L) of potassium chloride. Plants were grown in a 16-/8-h light/dark cycle at 22°C/20°C, respectively, and 70% relative humidity. For the metal uptake assay and N estimation, seeds were germinated on a piece of nylon mesh over 0.5× MS medium and 2-week-old plants were transferred to magenta boxes containing 0.5× MS liquid medium buffered with 2 mM MES at pH 5.7. Plants were grown for 4 d at various concentrations of arsenite, and roots and shoots were harvested separately.

The *ggct2;1* T-DNA insertional mutant line (SALK_117578) was obtained from the ABRC. This T-DNA line was reported by ABRC as segregating for the insertion at the GGCT2;1 locus. Homozygosity was verified using the PCR method described at the SALK website (http://signal.salk.edu/gabout.html). *Arabidopsis* plants (wild-type Columbia-0) were transformed by vacuum infiltration as described by Bent et al. (1994) using the C58 strain of *Agrobacterium tumefaciens*. Transformed seeds were selected based on resistance to either hygromycin (15 mg/L) for the ACT2pt/At-GGCT construct or kanamycin (30 mg/L) for the AtGGCTp-GUS construct.

Gene Isolation and Plasmid Transformation

The *Arabidopsis* GGCT2;1 coding sequence was identified based on its similarity to the *Crambe abyssinica* ChaC protein sequence reported by Paulose et al. (2010). The sequence was amplified using the primers 5′-TACGTCGGTACCAAAACCATGGTTTTGTGGGTATTTGGA-3′ and 5′-TAGCTGCTCGAGTCATGATGCAAAGACCCGTTGA 3′ and ligated into a pGEM-T easy cloning vector (Promega). The insert was verified by

sequencing and then subcloned into either pYES2.0 or pYES3/CT (Invitrogen) at *Kpn*I and *Xho*I sites for heterologous expression in *Saccharomyces cerevisiae* strains and into a modified pCambia1300 binary vector at *Nco*I and *Xho*I sites for overexpression in plants. Modified pCambia1300 was prepared by inserting the *Arabidopsis ACT2* promoter-terminator cassette, *ACT2pt*, into the *Nco*I, *Xho*I, and *Hin*dIII restriction sites between the promoter and terminator sequences. For protein localization, *GGCT2;1* was amplified without the stop codon, fused in frame to the coding region of enhanced green fluorescent protein, and subcloned into modified pCambia1300 under the ACT2pt expression cassette.

For tissue-specific expression, a 1.0-kb sequence upstream of the *GGCT2;1* start codon was identified from the plant promoter database (Yamamoto and Obokata, 2008) and confirmed by verifying the *Arabidopsis* genome sequence in The Arabidopsis Information Resource (www.Arabidopsis.org). The sequence was amplified using the sense primer 5′-TAGCTGAAGCTTACCATCGATCGTTTCCTTTG-3′ and antisense primer 5′-TAGCTGGTCGACCTTTGATCCTTAGCCTCACAC-3′ and cloned into the *pBI101.1* vector (Clontech) at the *Hin*dIII and *Sal*I sites upstream of the GUS coding sequence.

Cloning and Functional Analysis of GGCT2;1 in *S. cerevisiae*

S. cerevisiae strains used were HD9 (MATα ura52 his6 leu2-3,112 hisΔ 200 trp1-901 lys2-801 suc2Δycf1:hisG acr3:URA3 fps1:leu2) and DTY167 (MATα ura52 his6 leu2-3,-112 hisΔ200 trp1-901 lys2-801 suc2-Δ, ycf1:hisG). The *S. cerevisiae* strains were transformed using the lithium acetate method (Knop et al., 1999), and transformed colonies were selected on SC medium (Sherman et al., 1986) lacking the appropriate amino acids (SC−). For estimation of As content, *S. cerevisiae* cells were grown in SC− medium with 1.6% Gal and 0.4% raffinose (w/v) as the carbon source. In parallel, cultures grown overnight in SC− medium were diluted to equal OD_{600} and used as inocula at different dilutions for growth assays on plates containing SC− with agar. In addition to the empty vector and untreated controls, As-/Cd-treated plates with Glc as the carbon source were also used as negative controls.

For the arsenite efflux assay, *S. cerevisiae* strains were allowed to accumulate As until the end of log phase in sodium arsenite–containing SC− medium, washed with chilled Tris-HCl buffer, pH 7.2, containing 0.5% NaCl, and resuspended in efflux buffer (2 mM MES, pH 5.5,1.6% Gal, and 0.4% raffinose) without sodium arsenite. Samples of cells and efflux buffer were drawn at 0, 15, 45, and 75 min to determine the concentration of As. The ratio of the total As content in the efflux buffer to the total As content in the cells at each time point was plotted.

RNA Isolation and RT-PCR Analysis

Total RNA from root and shoot tissues was extracted using the RNAeasy Plant Mini Kit (Qiagen), and cDNA was synthesized from total RNA using the Thermoscript RT-PCR kit (Invitrogen) following the manufacturers' protocol. For transcript expression analysis, a quantitative real-time PCR was performed following the instruction for Mastercycler ep realplex (Eppendorf) using gene-specific primers with ABsolute Blue QPCR SYBR Green Mix (Thermo Fisher Scientific). Relative expression level was calculated using the $2^{-\Delta\Delta CT}$ method (Livak and Schmittgen, 2001). For loss of gene-specific transcript analysis in T-DNA lines, a touchdown PCR was performed with an annealing temperature varying from 64 to 52°C for the first 10 cycles, followed by 18 cycles at a constant (52°C) annealing temperature. All reactions were done in triplicate, and the transcript levels relative to EF1α or ACT2 were reported as mentioned in figure legends.

Elemental Analysis in *S. cerevisiae* and Plant Samples

S. cerevisiae cells were washed with Tris-HCl buffer, pH 7.2, and the plant samples were washed with 0.01 N HCl followed by deionized water to remove any surface-deposited traces of metals. The *S. cerevisiae* and plant samples were heat dried at 75°C for 48 h, and the dried samples were digested with concentrated nitric acid for 48 h with constant shaking. Thirty percent hydrogen peroxide was added for complete mineralization, and samples were further digested for an additional 24 h. The digested samples were diluted and analyzed by ICP-MS (ELAN 6000 DRCe; Perkin-Elmer) for As and Cd content. Total N was estimated by the Kjeldahl method (Bradstreet, 1954) after mineralizing the dried tissues in concentrated sulfuric acid.

Measurement of GGCT Activity in Vitro

The GGCT2;1 coding sequence with a polyhistidine tag at the N terminus was expressed using the pET28a expression system (Novagen) by autoinduction as described by Studier (2005). The protein was then purified by affinity chromatography using Ni-nitrilotriacetic acid resin. Most of the recombinant proteins were in the inclusion bodies; hence, it was purified under denaturing conditions (6 M urea). The purified protein was renatured via dialysis with PBS, pH 7.4. Following dialysis, total protein was quantified by the Bradford method (Bradford, 1976). GGCT activity was determined in a 100-μL reaction with 100 mM Tris-HCl, 1 mM DTT, and 0.5 μg protein at 30°C. The reaction was stopped by adding 10 μL of 1.5 N HCl. 5-OP formed in the reaction was estimated by liquid chromatography–tandem mass spectrometry (LC-MS/MS) as described in the following section. K_m was calculated from a Hanes-Woolf plot.

Measurement of Cellular Levels of GSH and 5-OP

Total GSH content in *S. cerevisiae* cells and *Arabidopsis* was measured by reverse-phase HPLC using a modified procedure of Vatamaniuk et al. (2000). For GSH analysis, plants were grown on 0.5× MS on Petri plates for 18 d at normal growth conditions, as mentioned above, without any metal treatments. Briefly, plant tissues or *S. cerevisiae* cells were homogenized in liquid N_2 and extraction buffer containing 10 mM Tris-HCl, pH 8.0, 1 mM EDTA, pH 8.0, 1 mM DTT, and a protease inhibitor cocktail tablet (one tablet per 10 mL of buffer; Sigma-Aldrich). Tissue and cell debris were cleared by low-speed centrifugation at 3500*g* for 10 min at 4°C, the supernatant was collected, and the protein concentration in the supernatant was measured. Then, 5-sulfosalicylic acid was added to the extracts to a final concentration of 5%, and after a 5-min incubation on ice, precipitated proteins were pelleted by centrifugation at 18,000*g*, and the supernatants, which contained nonprotein thiols, were collected and used for GSH analyses. Aliquots of supernatants (100 μL) were filtered through a 0.22-μm filter and loaded onto an Econosphere C18, 150 × 4.6-mm RP-HPLC column (Alltech). The column was developed using a linear gradient of water/0.05% phosphoric acid and 2% acetonitrile/0.05% phosphoric acid with a flow rate of 1 mL/min. For quantitation of GSH, fractions (250 μL) were collected at 15-s intervals, and thiols were estimated spectrophotometrically at 412 nm after aliquots of the column fractions were reacted with 0.8 mM 5,5′-dithiobis-2-nitrobenzoic acid dissolved in 250 mM phosphate buffer, pH 7.6. Calibration was performed with authentic GSH. Fractions containing GSH were identified based on their comigration with commercially available GSH standards (Sigma-Aldrich).

The 5-OP contents in plant and *S. cerevisiae* samples were estimated using HPLC as described by Ohkama-Ohtsu et al. (2008) with minor modifications. For estimation of 5-OP contents, plant and *S. cerevisiae* samples were extracted with chilled 80% ethanol. The extracts were lyophilized and then dissolved in deionized or HPLC-grade water. After filtration, the redissolved samples were loaded onto a C18 column. The mobile phase was 2% perchloric acid, and a peak corresponding to 5-OP was observed at 220 nm at 5.0 min. The 5-OP content in plant and *S. cerevisiae* samples was calculated from a standard curve obtained by

loading known amounts of authentic 5-OP (Sigma-Aldrich), ranging from 1 nmol to 10,000 nmol per injection, onto a C18 column. Since this method could not detect 5-OP in mutant and wild-type plants, the plant samples were further analyzed by HPLC coupled to a triple quadrupole mass spectrometer with electrospray ionization by monitoring 130 to 84 mass-to-charge ratio transformation using the same method described in the following isotopic labeling studies.

Isotopic Labeling Studies

Plants were grown in 0.5 × MS liquid medium for 2 weeks and transferred to the modified 0.5 × MS medium with ^{15}N-labeled KNO_3 and 30 μM sodium arsenite. The roots were harvested at 0, 3, 6, and 12 h after changing to the modified MS medium, washed, and extracted with chilled 80% ethanol. The extract was centrifuged at 13,000*g*, and the lyophilized supernatant was redissolved in 10 mM Tris buffer. The prepared samples were analyzed by LC-MS/MS (Waters Micromass triple quad tandem mass spectrometer) as described by Eckstein et al. (2008). The liquid chromatography method included a stepwise gradient from 100% acidified water to 100% acidified acetonitrile. Both mobile phases contained heptafluorobutyric acid as ion pair reagent. The eluate was directed to the mass spectrometer through positive electrospray ionization. The ^{15}N-labeled Glu was detected by monitoring transformation of protonated labeled Glu to its fragments. Authentic standards from (Sigma-Aldrich) were used for quantification.

GUS Histochemical Analysis

Tissues from transgenic plants expressing GGCT2;1p-GUS were harvested and treated with 90% acetone for 20 min on ice. Tissues were stained overnight at 37°C in GUS staining solution containing 50 mM phosphate buffer, pH 7.2, 2 mM potassium ferrocyanide, 2 mM potassium ferricyanide, 0.2% Triton X-100, and 2 mM 5-bromo-4-chloro-indolyl glucuronide. Tissues were cleared with successive baths of increasing ethanol concentrations from 35 to 70%. Before adding 70% ethanol, tissues were treated with fixing buffer containing 5% formaldehyde, 50% ethanol, and 10% acetic acid, and micrographs were taken using the Olympus SZ60 microscope fitted with a Micropublisher 5.0 RTV charge-coupled device camera (QImaging).

Statistical Analysis

All statistical analyses were performed using SAS software (SAS version 9.1). For comparing treatments and control, the two-tailed Dunnett's *t* test (Dunnett, 1955) was performed after analysis of variance. In the case of multiple comparisons (N content and As/N molar ratio), Duncan's New Multiple range test (Duncan, 1957) was applied to separate the means.

Accession Numbers

Sequence data from this article can be found in the Arabidopsis Genome Initiative or GenBank/EMBL databases under the following locus ID or accession numbers: At-GGT1, At4g39640; At-GGT2, At4g39650; At-GGT4, At4g29210; At-GGCT1, At1g44790, NP_564490; At-GGCT2;1, At5g26220, NP_197994; At-GGCT2;2, At4g31290, NP_567871; Os-ChaC1, NP_001052924; Os-ChaC2, NP_001046811; Ec-ChaC, NP_415736; Sc-ChaC, P32656; Mm-ChaC1, NP_081205; Mm-ChaC2, NP_080803; Hs-ChaC1, NP_077016; Hs-ChaC2, NP_001008708; Hs-GGCT(C7orf24), NM_001199817; *Arabidopsis ACT2*, U41998.1; *Arabidopsis Elongation factor* (*EF1*α) AK226349.1; T-DNA insertion mutant (in the seventh exon) *ggct2;1*, SALK_117578; and T-DNA insertion in the 3′ untranslated region of *GGCT2;1*, SALK_036650.

Supplemental Data

The following materials are available in the online version of this article.

Supplemental Figure 1. Amino Acid Sequences of Putative GGCT Proteins with ChaC-Like Domains from Various Organisms Aligned with Human GGCT.

Supplemental Figure 2. Phylogenetic Analysis of Putative GGCT Proteins with ChaC-Like Domains from Various Organisms.

Supplemental Figure 3. Arsenic- and Cadmium-Tolerant Phenotype of a Second *ggct2;1* T-DNA Insertional Mutant (SALK_036650).

Supplemental Figure 4. RT-PCR Showing Higher Levels of *GGCT2;1* mRNA Transcripts in the GGCT2;1 Overexpression Lines.

Supplemental Figure 5. Localization of the GGCT2;1-GFP Fusion Protein in *Arabidopsis* Protoplasts.

Supplemental Methods 1. Subcellular Localization of GGCT2;1 in *Arabidopsis*

Supplemental Data Set 1. Text File of the Sequences and Alignment used for the Phylogenetic Analysis Shown in Supplemental Figure 2.

ACKNOWLEDGMENTS

We thank Kathleen Farquharson for critical reading and editing of the article and for valuable suggestions. We thank Richard B. Meagher for providing the ACT2pt construct and for critical reading and valuable suggestions to improve this article. We also thank Barry P. Rosen for providing the HD9 and DTY167 *S. cerevisiae* mutant strains. We thank the ABRC for providing the *Arabidopsis* mutant seeds. We also thank Alice Cheung and Chao Li for support of green fluorescent protein work, David Reckhow and John Tobiason for kindly allowing the use of ICP-MS and LC-MS/MS devices, and Allen Barker for support in nitrogen analysis. This work was supported by a Hatch grant (MAS00401) from the USDA to the Stockbridge School of Agriculture, University of Massachusetts, Amherst, and partly by the Consortium of Plant Biotech Research (GO12026-273).

AUTHOR CONTRIBUTIONS

O.P.D. supervised project. O.P.D. and B.P. designed experiments, analyzed data, and wrote the article. B.P. performed functional and genetic studies in yeast and plants, metabolite analysis, and biochemical characterization. S.C. participated in gene expression analysis. J.C. participated in mutant studies. H.J. and O.V. participated in thiol measurements in yeast and plants.

Received March 25, 2013; revised August 31, 2013; accepted October 17, 2013; published November 8, 2013.

REFERENCES

Ayotte, J.D., Montgomery, D.L., Flanagan, S.M., and Robinson, K.W. (2003). Arsenic in groundwater in eastern New England: Occurrence, controls, and human health implications. Environ. Sci. Technol. **37:** 2075–2083.

Bent, A.F., Kunkel, B.N., Dahlbeck, D., Brown, K.L., Schmidt, R., Giraudat, J., Leung, J., and Staskawicz, B.J. (1994). *RPS2* of *Arabidopsis thaliana*: A leucine-rich repeat class of plant disease resistance genes. Science **265:** 1856–1860.

Bhatia, N.P., Nkang, A.E., Walsh, K.B., Baker, A.J.M., Ashwath, N., and Midmore, D.J. (2005). Successful seed germination of the nickel hyperaccumulator *Stackhousia tryonii*. Ann. Bot. (Lond.) **96:** 159–163.

Bogdanova, N., and Hell, R. (1997). Cysteine synthesis in plants: Protein-protein interactions of serine acetyltransferase from *Arabidopsis thaliana*. Plant J. **11:** 251–262.

Bradford, M.M. (1976). A rapid and sensitive method for the quantitation of microgram quantities of protein utilizing the principle of protein-dye binding. Anal. Biochem. **72:** 248–254.

Bradstreet, R.B. (1954). Kjeldahl method for organic nitrogen. Anal. Chem. **26:** 185–187.

Cobbett, C.S., May, M.J., Howden, R., and Rolls, B. (1998). The glutathione-deficient, cadmium-sensitive mutant, *cad2-1*, of *Arabidopsis thaliana* is deficient in glutamylcysteine synthetase. Plant J. **16:** 73–78.

Dhankher, O.P. (2005). Arsenic metabolism in plants: An inside story. New Phytol. **168:** 503–505.

Dhankher, O.P., Li, Y., Rosen, B.P., Shi, J., Salt, D., Senecoff, J.F., Sashti, N.A., and Meagher, R.B. (2002). Engineering tolerance and hyperaccumulation of arsenic in plants by combining arsenate reductase and γ-glutamylcysteine synthetase expression. Nat. Biotechnol. **20:** 1140–1145.

Dhankher, O.P., Rosen, B.P., McKinney, E.C., and Meagher, R.B. (2006). Hyperaccumulation of arsenic in the shoots of Arabidopsis silenced for arsenate reductase (ACR2). Proc. Natl. Acad. Sci. USA **103:** 5413–5418.

Duncan, D.B. (1957). Multiple range tests for correlated and heteroscedastic means. Biometrics **13:** 164–176.

Dunnett, C.W. (1955). A multiple comparison procedure for comparing several treatments with a control. J. Am. Stat. Assoc. **50:** 1096–1121.

Eckstein, J.A., Ammerman, G.M., Reveles, J.M., and Ackermann, B.L. (2008). Analysis of glutamine, glutamate, pyroglutamate, and GABA in cerebrospinal fluid using ion pairing HPLC with positive electrospray LC/MS/MS. J. Neurosci. Methods **171:** 190–196.

Ellis, D.R., Gumaelius, L., Indriolo, E., Pickering, I.J., Banks, J.A., and Salt, D.E. (2006). A novel arsenate reductase from the arsenic hyperaccumulating fern *Pteris vittata*. Plant Physiol. **141:** 1544–1554.

Forde, B.G., and Lea, P.J. (2007). Glutamate in plants: Metabolism, regulation, and signalling. J. Exp. Bot. **58:** 2339–2358.

Fricker, M.D., May, M., Meyer, A.J., Sheard, N., and White, N.S. (2000). Measurement of glutathione levels in intact roots of *Arabidopsis*. J. Microsc. **198:** 162–173.

Geiger, M., Walch-Liu, P., Engels, C., Harnecker, J., Schulze, E.D., Ludewig, F., Sonnewald, U., Scheible, W.R., and Stitt, M. (1998). Enhanced carbon dioxide leads to a modified diurnal rhythm of nitrate reductase activity in older plants, and a large stimulation of nitrate reductase activity and higher levels of amino acids in young tobacco plants. Plant Cell Environ. **21:** 253–268.

Ghosh, M., Shen, J., and Rosen, B.P. (1999). Pathways of As(III) detoxification in *Saccharomyces cerevisiae*. Proc. Natl. Acad. Sci. USA **96:** 5001–5006.

Gibon, Y., Usadel, B., Blaesing, O.E., Kamlage, B., Hoehne, M., Trethewey, R., and Stitt, M. (2006). Integration of metabolite with transcript and enzyme activity profiling during diurnal cycles in *Arabidopsis* rosettes. Genome Biol. **7:** R76.

Griffith, O.W., Bridges, R.J., and Meister, A. (1978). Evidence that the gamma-glutamyl cycle functions in vivo using intracellular glutathione: Effects of amino acids and selective inhibition of enzymes. Proc. Natl. Acad. Sci. USA **75:** 5405–5408.

Grzam, A., Martin, M.N., Hell, R., and Meyer, A.J. (2007). γ-Glutamyl transpeptidase GGT4 initiates vacuolar degradation of glutathione S-conjugates in *Arabidopsis*. FEBS Lett. **581:** 3131–3138.

Ha, S.B., Smith, A.P., Howden, R., Dietrich, W.M., Bugg, S., O'Connell, M.J., Goldsbrough, P.B., and Cobbett, C.S. (1999). Phytochelatin synthase genes from *Arabidopsis* and the yeast *Schizosaccharomyces pombe*. Plant Cell **11:** 1153–1164.

Hanson, A.D., and Gregory, J.F., III., (2002). Synthesis and turnover of folates in plants. Curr. Opin. Plant Biol. **5:** 244–249.

Hartley-Whitaker, J., Ainsworth, G., Vooijs, R., Ten Bookum, W., Schat, H., and Meharg, A.A. (2001). Phytochelatins are involved in differential arsenate tolerance in *Holcus lanatus*. Plant Physiol. **126:** 299–306.

Howden, R., Goldsbrough, P.B., Andersen, C.R., and Cobbett, C.S. (1995). Cadmium-sensitive, *cad1* mutants of *Arabidopsis thaliana* are phytochelatin deficient. Plant Physiol. **107:** 1059–1066.

Jaspers, C., Gigot, D., and Penninckx, M.J. (1985). Pathway of glutathione degradation in the yeast *Saccharomyces cerevisiae*. Phytochemistry **24:** 703–707.

Jócsák, I., Végvári, G., and Droppa, M. (2005). Heavy metal detoxification by organic acids in barley seedlings. Acta Biol. Szegediensis **49:** 99–101.

Knop, M., Siegers, K., Pereira, G., Zachariae, W., Winsor, B., Nasmyth, K., and Schiebel, E. (1999). Epitope tagging of yeast genes using a PCR-based strategy: More tags and improved practical routines. Yeast **15** (10B)**:** 963–972.

Krämer, U., Pickering, I.J., Prince, R.C., Raskin, I., and Salt, D.E. (2000). Subcellular localization and speciation of nickel in hyperaccumulator and non-accumulator *Thlaspi* species. Plant Physiol. **122:** 1343–1353.

Kumar, A., and Bachhawat, A.K. (2010). *OXP1/YKL215c* encodes an ATP-dependent 5-oxoprolinase in *Saccharomyces cerevisiae*: Functional characterization, domain structure and identification of actin-like ATP-binding motifs in eukaryotic 5-oxoprolinases. FEMS Yeast Res. **10:** 394–401.

Kumar, A., Tikoo, S., Maity, S., Sengupta, S., Sengupta, S., Kaur, A., and Bachhawat, A.K. (2012). Mammalian proapoptotic factor ChaC1 and its homologues function as γ-glutamyl cyclotransferases acting specifically on glutathione. EMBO Rep. **13:** 1095–1101.

Li, J.Y., et al. (2010). The *Arabidopsis* nitrate transporter NRT1.8 functions in nitrate removal from the xylem sap and mediates cadmium tolerance. Plant Cell **22:** 1633–1646.

Li, Y., Dhankher, O.P., Carreira, L., Lee, D., Chen, A., Schroeder, J.I., Balish, R.S., and Meagher, R.B. (2004). Overexpression of phytochelatin synthase in *Arabidopsis* leads to enhanced arsenic tolerance and cadmium hypersensitivity. Plant Cell Physiol. **45:** 1787–1797.

Li, Z.S., Szczypka, M., Lu, Y.P., Thiele, D.J., and Rea, P.A. (1996). The yeast cadmium factor protein (YCF1) is a vacuolar glutathione S-conjugate pump. J. Biol. Chem. **271:** 6509–6517.

Liu, J., and Rosen, B.P. (1997). Ligand interactions of the ArsC arsenate reductase. J. Biol. Chem. **272:** 21084–21089.

Liu, Z., Shen, J., Carbrey, J.M., Mukhopadhyay, R., Agre, P., and Rosen, B.P. (2002). Arsenite transport by mammalian aquaglyceroporins AQP7 and AQP9. Proc. Natl. Acad. Sci. USA **99:** 6053–6058.

Livak, K.J., and Schmittgen, T.D. (2001). Analysis of relative gene expression data using real-time quantitative PCR and the $2-\Delta\Delta CT$ method. Methods **25:** 402–408.

Marrs, K.A. (1996). The functions and regulation of glutathione S transferases in plants. Annu. Rev. Plant Physiol. Plant Mol. Biol. **47:** 127–158.

Martin, M.N., Saladores, P.H., Lambert, E., Hudson, A.O., and Leustek, T. (2007). Localization of members of the γ-glutamyl transpeptidase family identifies sites of glutathione and glutathione S-conjugate hydrolysis. Plant Physiol. **144:** 1715–1732.

Marty, L., Siala, W., Schwarzländer, M., Fricker, M.D., Wirtz, M., Sweetlove, L.J., Meyer, Y., Meyer, A.J., Reichheld, J.P., and Hell, R.

(2009). The NADPH-dependent thioredoxin system constitutes a functional backup for cytosolic glutathione reductase in *Arabidopsis*. Proc. Natl. Acad. Sci. USA **106:** 9109–9114.

Matt, P., Geiger, M., Walch-Liu, P., Engels, C., Krapp, A., and Stitt, M. (2001). The immediate cause of the diurnal changes of nitrogen metabolism in leaves of nitrate-replete tobacco: A major imbalance between the rate of nitrogen reduction and the rates of nitrate uptake and ammonium metabolism during the first part of the light period. Plant Cell Environ. **24:** 177–190.

Maughan, S.C., et al. (2010). Plant homologs of the *Plasmodium falciparum* chloroquine-resistance transporter, PfCRT, are required for glutathione homeostasis and stress responses. Proc. Natl. Acad. Sci. USA **107:** 2331–2336.

Mazelis, M., and Creveling, R.K. (1978). 5-Oxoprolinase (L-pyroglutamate hydrolase) in higher plants: Partial purification and characterization of the wheat germ enzyme. Plant Physiol. **62:** 798–801.

Meister, A. (1988). Glutathione metabolism and its selective modification. J. Biol. Chem. **263:** 17205–17208.

Meister, A. (1974). Glutathione synthesis. In The Enzymes, P.D. Boyer, ed (New York: Academic Press), pp. 671–697.

Miflin, B.J., and Lea, P.J. (1976). Review: The pathway of nitrogen assimilation in plants. Phytochemistry **15:** 873–885.

Murashige, T., and Skoog, F. (1962). A revised medium for rapid growth and bioassays with tobacco tissue cultures. Physiol. Plant. **15:** 473–497.

Oakley, A.J., Yamada, T., Liu, D., Coggan, M., Clark, A.G., and Board, P.G. (2008). The identification and structural characterization of C7orf24 as γ-glutamyl cyclotransferase. An essential enzyme in the γ-glutamyl cycle. J. Biol. Chem. **283:** 22031–22042.

Ohkama-Ohtsu, N., Oikawa, A., Zhao, P., Xiang, C., Saito, K., and Oliver, D.J. (2008). A gamma-glutamyl transpeptidase-independent pathway of glutathione catabolism to glutamate via 5-oxoproline in Arabidopsis. Plant Physiol. **148:** 1603–1613.

Pasternak, M., Lim, B., Wirtz, M., Hell, R., Cobbett, C.S., and Meyer, A.J. (2008). Restricting glutathione biosynthesis to the cytosol is sufficient for normal plant development. Plant J. **53:** 999–1012.

Paulose, B., Kandasamy, S., and Dhankher, O.P. (2010). Expression profiling of *Crambe abyssinica* under arsenate stress identifies genes and gene networks involved in arsenic metabolism and detoxification. BMC Plant Biol. **10:** 108.

Polhuijs, M., Lankhaar, G., and Mulder, G.J. (1992). Relationship between glutathione content in liver and glutathione conjugation rate in the rat in vivo. Effect of buthionine sulphoximine pretreatment on conjugation of the two 2-bromoisovalerylurea enantiomers during intravenous infusion. Biochem. J. **285:** 401–404.

Rennenberg, H., Steinkamp, R., and Kesselmeier, J. (1981). 5-Oxoprolinase in *Nicotiana tabacum*: Catalytic properties and subcellular localization. Physiol. Plant. **62:** 211–216.

Sagner, S., Kneer, R., Wanner, G., Cosson, J.P., Deus-Neumann, B., and Zenk, M.H. (1998). Hyperaccumulation, complexation and distribution of nickel in *Sebertia acuminata*. Phytochemistry **47:** 339–347.

Sherman, F., Fink, G.R., and Hicks, J.B. (1986). Methods in Yeast Genetics. (Cold Spring Harbor, NY: Cold Spring Harbor Laboratory Press).

Shi, W., Dong, J., Scott, R.A., Ksenzenko, M.Y., and Rosen, B.P. (1996). The role of arsenic-thiol interactions in metalloregulation of the *ars* operon. J. Biol. Chem. **271:** 9291–9297.

Srivastava, S., and D'Souza, S.F. (2009). Increasing sulfur supply enhances tolerance to arsenic and its accumulation in *Hydrilla verticillata* (Lf.) Royle. Environ. Sci. Technol. **43:** 6308–6313.

Steinkamp, R., and Rennenberg, H. (1987). γ-Glutamylcyclotransferase in tobacco suspension cultures: Catalytic properties and subcellular localization. Physiol. Plant. **69:** 499–503.

Studier, F.W. (2005). Protein production by auto-induction in high density shaking cultures. Protein Expr. Purif. **41:** 207–234.

Suzuki, K.T., Tomita, T., Ogra, Y., and Ohmichi, M. (2001). Glutathione-conjugated arsenics in the potential hepato-enteric circulation in rats. Chem. Res. Toxicol. **14:** 1604–1611.

Tseng, C.H. (2009). A review on environmental factors regulating arsenic methylation in humans. Toxicol. Appl. Pharmacol. **235:** 338–350.

Vatamaniuk, O.K., Mari, S., Lu, Y.P., and Rea, P.A. (2000). Mechanism of heavy metal ion activation of phytochelatin (PC) synthase: Blocked thiols are sufficient for PC synthase-catalyzed transpeptidation of glutathione and related thiol peptides. J. Biol. Chem. **275:** 31451–31459.

Verbruggen, N., Hermans, C., and Schat, H. (2009). Mechanisms to cope with arsenic or cadmium excess in plants. Curr. Opin. Plant Biol. **12:** 364–372.

Wachter, A., Wolf, S., Steininger, H., Bogs, J., and Rausch, T. (2005). Differential targeting of GSH1 and GSH2 is achieved by multiple transcription initiation: Implications for the compartmentation of glutathione biosynthesis in the Brassicaceae. Plant J. **41:** 15–30.

Xiang, C., and Oliver, D.J. (1998). Glutathione metabolic genes coordinately respond to heavy metals and jasmonic acid in *Arabidopsis*. Plant Cell **10:** 1539–1550.

Yamamoto, Y.Y., and Obokata, J. (2008). ppdb: A plant promoter database. Nucleic Acids Res. **36** (Database issue)**:** D977–D981.

Yaronskaya, E., Vershilovskaya, I., Poers, Y., Alawady, A.E., Averina, N., and Grimm, B. (2006). Cytokinin effects on tetrapyrrole biosynthesis and photosynthetic activity in barley seedlings. Planta **224:** 700–709.

Zhu, Y.L., Pilon-Smits, E.A.H., Tarun, A.S., Weber, S.U., Jouanin, L., and Terry, N. (1999). Cadmium tolerance and accumulation in Indian mustard is enhanced by overexpressing gamma-glutamylcysteine synthetase. Plant Physiol. **121:** 1169–1178.